Journal of Applied Polymer Science

WILEY

Applied Polymer SCIENCE

RESEARCH ARTICLE

Enhancing Oil Rejection in PVDF and PSF membranes: The Role of SiO_2 NPs

Dilek Senol-Arslan[1] | Ayse Gul[2]

[1]Department of Materials Science and Nanotechnology Engineering, Abdullah Gül University, Kayseri, Turkey | [2]Department of Civil Engineering, Abdullah Gül University, Kayseri, Turkey

Correspondence: Dilek Senol-Arslan (dilek.senol@agu.edu.tr)

Received: 15 July 2024 | **Revised:** 22 November 2024 | **Accepted:** 30 November 2024

Funding: The authors received no specific funding for this work.

ABSTRACT

Oily water negatively affects both land and marine ecosystems. To combat this, membrane production can effectively treat oil waste and recycle over 90% of it. This study compares the influence of SiO_2 nanoparticles on oil rejection in two types of membranes: polyvinylidene fluoride (PVDF) and polysulfone (PSF). The SiO_2 NPs are characterized by FTIR, SEM analysis, and zeta potential measurements. SiO_2 NPs embedded PSF and PVDF membranes were characterized by FTIR, SEM analysis, contact angle, water permeability, oil rejection measurements, and recycling experiments. The results of the experiments showed that oil rejection reached maximum values of 92.2% for 2 wt% PSF/SiO_2, and 94.1% for 2 wt% PVDF/SiO_2 membranes. The experimental results demonstrate that the incorporation of SiO_2 nanoparticles enhances the oil rejection efficiency of two distinct membrane types, exhibiting notable performance disparities contingent on the selected membrane material. This methodology achieves a recycling rate of over 90% for oil waste, signifying a substantial advancement in environmental protection and sustainable development. Consequently, the membrane production technique is regarded as an efficacious approach for the management and recycling of oil waste.

1 | Introduction

Oil–water separation is becoming increasingly important in a wide range of applications such as textile [1], food, [2] leather [3], metal processing [4], oil and gas [5], and mining [6] are among the industries that generate a significant amount of industrial oily wastewater. The oil sector is prone to oil spills during the phases of exploration and production [7], refining [8], and transportation [9] which can have detrimental effects on the environment and the economy [10–12]. Even though oil spill occurrences have an adverse effect on public health and the environment, less than 10% of the oil that enters the oceans comes from them. The discharge of oily wastewater, such as brine, into natural water bodies can significantly degrade water quality, leading to a variety of environmental and ecological problems [13–15].

Before being discharged into the environment, oily wastewater must first go through an efficient treatment procedure, which is a highly desired and urgent mitigation of the increasing freshwater resource problem and environmental deterioration. Therefore, the development of efficient treatment techniques for removing oil from oily wastewater is crucial for the appropriate management of all these problems [16, 17].

Absorption, adsorption, membrane separation, biological treatment, electrocoagulation [18], air floatation, and heterogeneous photocatalysis are some of the technologies used for the treatment of oily waters [19]. Technologies such as coagulation, air flotation, gravity separation, sedimentation, electrolytic separation, and biological methods are infrequently utilized because of their elevated operational expenses, ineffective oil–water separation [20–22]. However, oily wastewater

is successfully separated using microfiltration and ultrafiltration membranes without the use of chemicals or the production of sludge [23]. Additionally, membrane technology is a very effective option for water treatment that provides better water quality at a cheap cost. Its compact design saves space, and the system's maintenance requirements are simple, making it appealing for a wide range of water purification applications [24, 25]. Membrane technology is considered as an eco-friendly and highly effective separation method with a simple operation and filtering effect on tiny droplets. But oils and surfactants can readily clog pores of the membranes during the separation process, reducing separation efficiency. Nanocomposite membranes, also known as mixed matrix membranes with nanoparticles, have been shown to improve membrane hydrophilicity and antifouling properties. This approach offers a simple solution to improve membrane performance in a variety of filtration applications [24].

A series of recent studies have focused on the hydrophilic modification of membrane surfaces as a means of reducing membrane fouling in the treatment of oil/water mixtures. In oil-aqueous mixtures, hydrophilic membranes have been found to be an effective solution for selective oil and water phase separation, offering high separation efficiency and anti-oil fouling properties. Hydrophilic membranes can be used for filtration [26, 27], gas separation [28], membrane gas absorption [29], pervaporation [30], and membrane distillation [31].

Recently, the development of hydrophilic membranes for the separation of oil and water has received more attention. Liu et al. synthesized a hydrophilic PES membrane; Ebrahimi et al. developed hydrophilic electrospun membrane decorated with SiO_2 nanoparticles; Yao et al. created ultra-selective microfiltration SiO_2/carbon membranes; Zakuwan et al. produced functional hydrophilic membrane for oil–water separation. All results showed that high removal efficiency was obtained with hydrophobic membranes (97%, 98%, 99.9%, 98%) [32–35].

The performance of microfiltration/ultrafiltration membranes can be improved by introducing particular modifications in the base materials. Nanomaterials are also fixed on membranes because of their special properties, which improves the effectiveness of such membranes for oil/water separation [36]. Using simple techniques, many nanoparticles can easily form super-hydrophobic micro/nano structures on surfaces [37]. Adding additives into casting solution was an effective method to prepare composite membrane. Among various nanoparticles such as clay [38], SiO_2 [20, 39], TiO_2 [40], GO [16], chitosan [41, 42] are embedded into the membrane to enhance the membrane's properties for oil/water separation. Silica has highly attracted a lot of interest among them as a type of nanoparticle.

Polymeric membranes, including polyvinylidene fluoride (PVDF), polytetrafluoroethylene (PTFE), polypropylene (PP), and polysulfone (PSF), have been widely used as effective substrate materials for the separation of stable oil/water emulsions because of their appropriate porosity, remarkable flexibility, and durability [16, 43].

Due to their excellent physical and chemical stability and low surface energy, PVDF-MF membranes are vulnerable to significant membrane fouling in oily water treatment, which eventually results in performance loss. Additionally, PVDF is one of the commonly used polymers for oil–water separation. Due to its advantageous characteristics, for instance, attributes such as low surface energy, high mechanical strength, and robust physical and chemical stability are noteworthy [44].

Physical mixing and chemical grafting are used to minimize the fouling effect. Due to its ease of preparation using the phase separation method in a single step and efficiency in enhancing the anti-fouling performance, physical blending, in particular by inorganic nanoparticles (silica (SiO_2), titanium dioxide) into the PVDF membrane matrix, has attracted significant attention [39, 45].

PSF is another polymer employed for oil–water separation due to low cost, superior film forming ability, and strong chemical and thermal stability. However, due to its hydrophobic nature, the permeability of the membrane frequently decreases, leading to significant membrane fouling. To enhance the hydrophobicity of the PSF membrane using nanoparticles, modifications are necessary [46].

Recent membrane studies with SiO_2 showed that the addition of SiO_2 NPs resulted in the best oil/water separation with rejection above 90% [32, 47, 48]. Also, the separation efficiency did not significantly change after 10 cycles of separation. It is clear from recent studies that silica nanoparticles are also promising for producing super hydrophobic membrane for effective oil–water separation.

The challenge of improving oil rejection in polymeric membranes has become increasingly critical due to the growing demand for effective water treatment technologies. This study presents a novel approach by investigating and comparing the role of SiO_2 NPs in enhancing the oil rejection capabilities of PVDF and PSF membranes without using any surfactant. Unlike previous studies which have mostly focused on changing membrane structure or surface chemistry, our research shows how the addition of SiO_2 NPs can considerably increase membrane hydrophilicity and antifouling capabilities. Since it is the first comparative research on the oil-rejection performance of PVDF and PSF membranes with and without SiO_2 NPs, this article will contribute to the literature.

2 | Materials and Methods

2.1 | Materials

PVDF and PSF (with an average Mw = 60,000 Da) were supplied from Acros Organics (Geel, Belgium), DMF (N,N-Dimethylformamide) was obtained from Merck (Darmstadt, Germany). SiO_2 NPs (SiO_X, 99.5+%, 15–20 nm, S-type, spherical, nonporous, and amorphous) were purchased from Nanografi. Waste hydraulic oil was collected from garages.

3 | Methods

3.1 | Membrane Fabrication

Dope solution is prepared using PVDF and PSF as a polymer, DMF (solvent) and SiO_2 NPs. First, the SiO_2 NPs was stirred in DMF with a stirrer and then the polymer is added slowly. Stirred until the polymer is completely dissolved. The resulting dope suspension is sonicated to homogeneously disperse the silica particles. Schematic representation of the fabrication of SiO_2 NPs embedded PVDF and PSF membranes presented in Figure 1. The components of the dope solution are presented in Tables 1 and 2.

3.1.1 | Membrane Filtration Tests

3.1.1.1 | Preparation of Oil-in-Water Emulsions. Grease and oil concentrations in oily wastewaters can reach 5495 mg/L [49]. A 5 g/L solution was produced to create an oil-in-water emulsion model. A homogeneous solution (5 g/L) was obtained by mixing aging hydraulic oil and distilled water vigorously for 1 h to create the oil-in-water emulsion model.

The oil concentration was determined in the permeate using an Hach UV–visible spectrophotometer at 387 nm. The value of oil concentration can be calculated by converting the absorbance of the fluid under test.

The basic separation capabilities (water flux and rejection) of the membranes evaluated using a dead-end stirred cell filtration system (Sterlitech, HP4750). A 300 mL-capacity filtration cell is used, and it is connected to a nitrogen gas cylinder. The system's effective membrane area is 14.6 cm^2. For the filtering test, DI water has been the feed solution, and nitrogen gas was used to pressurize the feed side of the system. Transmembrane pressure (TMP) for PVDF; PVDF/SiO_2 and PSF; PSF/SiO_2 membranes in the water filtration test was 5 and 10 bars, the stirring speed was 300 rpm, and the temperature maintained

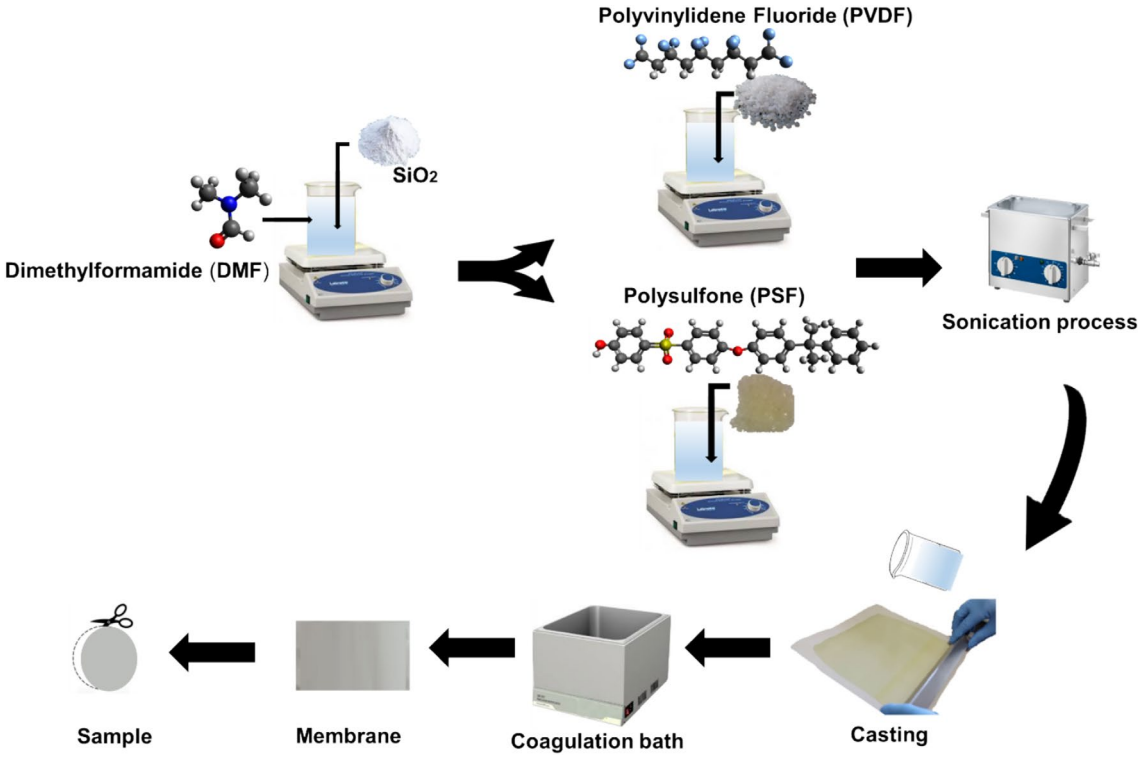

FIGURE 1 | Schematic representation of the fabrication of SiO_2 NPs embedded PVDF and PSF membranes. [Color figure can be viewed at wileyonlinelibrary.com]

TABLE 1 | The components of the dope solution for PVDF membrane.

Membrane	PVDF (wt%)	DMF (wt%)	SiO_2 NPs (wt%)
PVDF	15	85	—
PVDF + 1% SiO_2	14	85	1
PVDF + 2% SiO_2	13	85	2
PVDF + 3% SiO_2	12	85	3

TABLE 2 | The components of the dope solution for PSF membrane.

Membrane	PSF (wt%)	DMF (wt%)	SiO_2 NPs (wt%)
PSF	20	80	—
PSF + 1% SiO_2	19	85	1
PSF + 2% SiO_2	18	85	2
PSF + 3% SiO_2	17	85	3

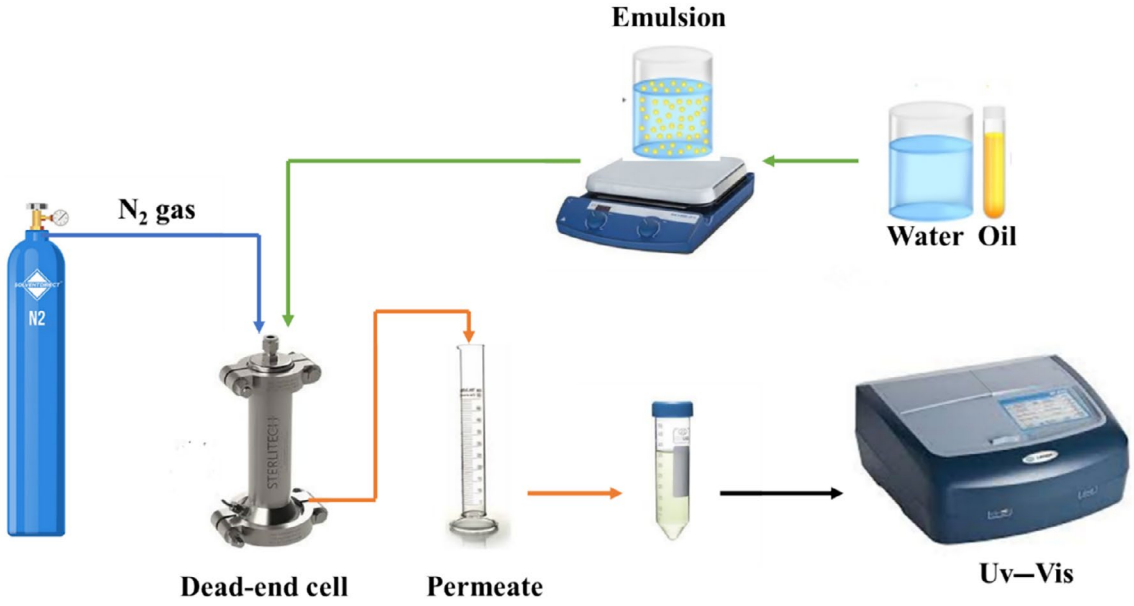

FIGURE 2 | Schematic representation of the oil rejection experiments. [Color figure can be viewed at wileyonlinelibrary.com]

at 25°C. Equation (1) will be used to determine water fluxes of the membranes.

3.1.1.2 | Evaluation of Oil Separation Performance. A dead-end stirred cell filtration system is employed to assess the efficiency of PVDF and PSF membranes for separation. Aging hydraulic oil used for preparation of the synthetic oil/water emulsion. At a stirring speed of 250 rpm and a TMP of 5 and 10 bar, the oil rejection tests were carried out in the dead-end filtering module (Figure 2). The membranes filtered the pure water for 20 min (2 bar). After that, a 250 mL sample of the emulsion was added and run through the membranes on the vacuum filtering system. In order to calculate the separation flux (J) and rejection ratio (η), flux decay ratio (DR) and flux recovery ratio (FRR) the formulas shown below. Samples of wastewater were tested for the presence of oil at a wavelength of 387 nm using UV-visible spectroscopy.

$$J = \frac{V}{A \times t} \tag{1}$$

$$\%\eta = 1 - \frac{C}{C_0} \times 100 \tag{2}$$

$$\mathrm{DR} = \frac{J - J_1}{J} \times 100 \tag{3}$$

$$\mathrm{FRR} = \frac{J_2}{J} \times 100 \tag{4}$$

where J represents the water flux (L/m^{2}h), V represents the permeate volume (L), A represents the effective membrane area (m^2), and t represents time (h). C_0 (g/L) and C (g/L) represent the oil concentrations in the emulsion before and after filtering, respectively. J_1 (L/m^{2}h) is the oil/water emulsion flux, and J_2 (L/m^{2}h) cleaned membrane water flux.

3.2 | Separation Cycling Experiments

Ten separation cycling tests were conducted to determine the membrane's durability and anti-fouling capabilities with PSF + SiO_2(wt 2%) and PVDF+SiO_2(wt 2%). Every cycle includes both the washing and separating processes. Before starting the next cycle, the membrane is repeatedly cleaned with deionized water to eliminate any remaining oil.

3.3 | Zeta Potential Measurements

The value of the zeta potential of the SiO_2 Nps samples was determined using Nano ZS90 (Malvern, UK) equipment. SiO_2 NPs solution was prepared with a solid concentration of 1% by weight. pH profile adjusted with 0.1 M HCl and NaOH.

Each data point represents the average of approximately 20 measurements taken at room temperature, all of which were carried out at room temperature.

3.4 | Contact Angle Measurements

The sessile drop method was used to measure the water contact angle to determine the changes in surface hydrophilicity of each of the PVDF and PSF membranes after the addition of SiO_2 Nps. The measurements were performed using Attention-Theta Lite, BiolinScientific, Finland.

3.5 | Fourier Transform Infrared Spectrophotometer Measurements

Fourier transform infrared (FT-IR) spectra were used to identify the functional properties of SiO_2 Nps and SiO_2 Nps

embedded PVDF and PSF membranes using an FT-IR spectrometer (Thermo Nicolet Avatar 370).

3.6 | Scanning Electron Microscopy

The structure and morphology of SiO_2 Nps and SiO_2 Nps embedded composite PVDF and PSF membranes at three different ratios (1%, 2%, and 3%) were examined using a scanning electron microscope (Zeiss Gemini) with a 10 kV applied voltage.

4 | Results and Discussion

4.1 | Zeta Potential

The determination of the surface electric charge of SiO_2 Nps in PVDF and PSF is crucial for optimizing membrane performance, increasing separation efficiency, controlling fouling, and ensuring membrane stability. Therefore, zeta potential analyses were carried out between pH 3 and 12 (Figure 3).

The zeta potential curve of SiO_2 NPs was analyzed, and it was found that it did not have a value for the isoelectric point (IEP). Its surface was negatively charged in all pH ranges, as shown in Figure 3.

SiO_2 NPs generally have a negative zeta potential due to surface silanol groups that can ionize and produce negative charges [50, 51].

4.2 | FT-IR

The chemical composition of oil, SiO_2 NPs, pristine PVDF and PSF, and SiO_2 NPs embedded nanocomposite membranes was evaluated using ATR-FTIR analysis (Figure 4). The use of FTIR analyses is crucial for the determination of the chemical interaction between the both PVDF and PSF membranes and SiO_2 NPs material, in addition to their efficiency in oil removal.

The FITR spectra of SiO_2 NPs exhibited the absorption peaks observed at 1080 and 802 cm^{-1} correspond to the Si—O—Si symmetric and asymmetric stretching vibrations, respectively. The absorption peak observed at 957 cm^{-1} was attributed to the stretching vibration of Si—OH bonds [52].

For PVDF, the peaks observed at 3367, 1403, and 1274 cm^{-1} can be attributed to the CH_2 stretching, deformation vibrations, and the CF_2 stretching vibration, respectively. The absorption peaks at 840, 877, 1072, 1179, and 1403 cm^{-1} indicate the presence of α and β phases. These are the two most common PVDF polymorphs [52–55].

The FTIR spectrum of the pristine PSF membrane exhibited peaks at 2968, 1240, and 1410–1585 cm^{-1}, which can be attributed to C—H, C—O—C, and C═C stretching vibrations, respectively. Symmetric (and asymmetric) stretching vibrations of the sulfonyl group (O═S═O) correspond to the peaks at 1013–1294 cm^{-1} [56, 57].

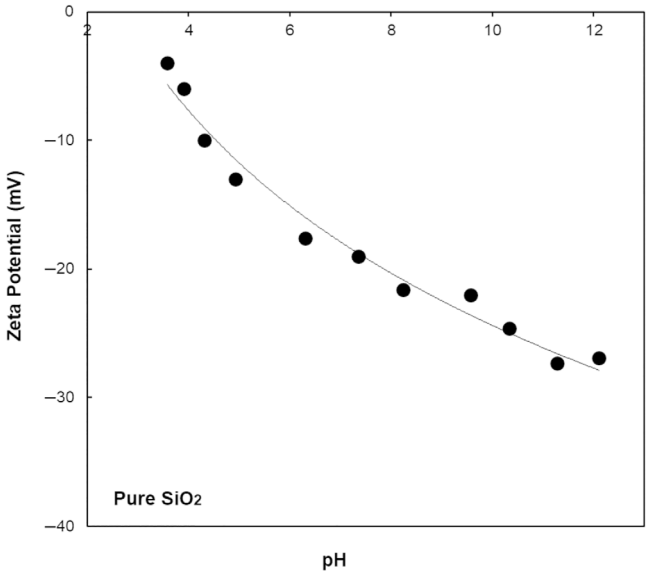

FIGURE 3 | Zeta potential of SiO_2 NPs.

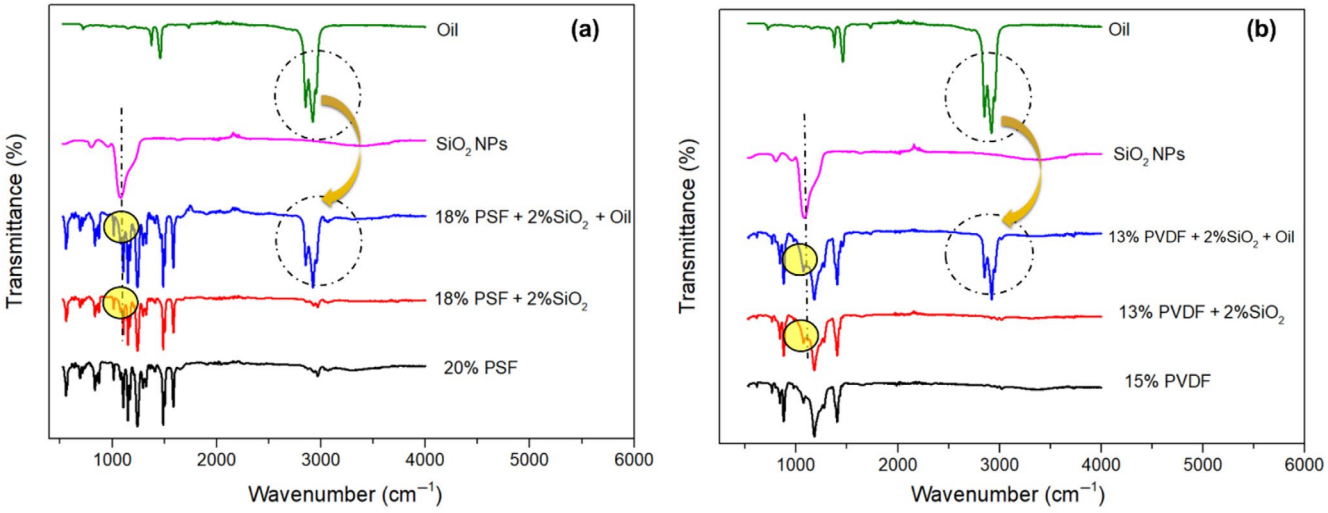

FIGURE 4 | (a) The FTIR spectra of oil, SiO_2 NPs, 20%PSF, 18%PSF + 2% SiO_2, and 18%PSF + 2%SiO_2 + oil. (b) FTIR spectra of oil, SiO_2 NPs, 15%PVDF, 13%PVDF+2% SiO_2, and 13%PVDF+2% SiO_2 + oil. [Color figure can be viewed at wileyonlinelibrary.com]

These results confirm the presence of silanol groups, siloxane linkages, and adsorbed water groups, as found in both SiO_2 NPs embedded PVDF and PSF membranes [58].

For oil, the peaks present at 3920 and 2852 cm^{-1} represent alkanes with a single bond. The carbonyl bond is observed at 1732 cm^{-1} [59].

4.3 | Contact Angle

The contact angles of the outer surfaces of the fabricated membranes (pristine PSF and pristine PVDF, at three different membrane concentrations of PVDF/SiO_2 NPs and PSF/SiO_2 NPs) were studied in detail (Figure 8a,b).

A comparison of the PSF membranes containing SiO_2 NPs with the pristine PSF membrane revealed a decline in the water contact angle from 79° to 67° (Figure 5a).

The maximum contact angle for the pristine PVDF membrane was found to be 73°. The PVDF/SiO_2 NPs membranes were observed to reduce the water contact angle down to 53° (Figure 5b).

As a result, the addition of SiO_2 NPs to PVDF and PSF membranes resulted in a slight decrease in water contact angles. This is attributed to the hydrophilic nature of SiO_2 NPs, which reduces the water contact angle of both membranes [60, 61].

4.4 | Scanning Electron Microscopy

In this study, scanning electron microscopy (SEM) was employed to provide detailed visualization of membrane surfaces at high magnifications. The cross-sectional SEM images of pristine PSF membrane the SiO_2/PSF membranes are presented in Figure 6c–e to illustrate the morphological changes in the substrate.

As can be seen in Figure 6a,c–e, all membranes exhibit a typical asymmetric membrane structure with a dense top layer and a substrate with finger-like pores.

As can be seen in Figure 6c–e, the impact of the addition of SiO_2 NPs was observed on the both hybrid membranes. It was observed that as the amount of SiO_2 NPs embedded on the membrane increased, the agglomeration of PSF/SiO_2 NPs membranes increased at the same rate.

Figure 7c–e shows that SiO_2 NPs are mainly deposited on the top surface of PVDF membranes. The amount of aggregates covering the pores on the membrane surface, which is affected by the amount of SiO_2 NPs on the surface, can be observed in all cross-sectional SEM images of modified PVDF membrane morphology.

Once all the results of the SEM have been evaluated in their entirety. In particular, the uniform pore structure and pore distribution in PSF and PVDF polymers provide evidence that the membranes are being produced successfully (Figures 6a and 7a). It was observed that surface morphology of both PSF and PVDF membrane containing SiO_2 NPs was suitable for oil/water separation.

4.5 | Membrane Filtration and Oil Rejection Experiments

The pristine water fluxes of PSF, PSF/1% SiO_2, PSF/2% SiO_2, and PSF/3% SiO_2 were determined at 10 bar using a dead-end filtration system. The results of pristine water flux from membranes are shown in Figure 8. The pristine water fluxes of PSF, PSF/1% SiO_2, PSF/2% SiO_2, and PSF/3% SiO_2 are 25.3, 45.6, 96.2, and 112.3 $L\,m^{-2}\,h^{-1}$, respectively. As can be seen, the water flux for PSF/ SiO_2 membrane increased from 25.3 to 112.3 $L\,m^{-2}\,h^{-1}$ by the addition of SiO_2 from 1% to 3%. Wu et al. discovered a similar outcome: Hybrid membranes with 0.3 wt% SiO_2 of nanoparticles have a higher water flux

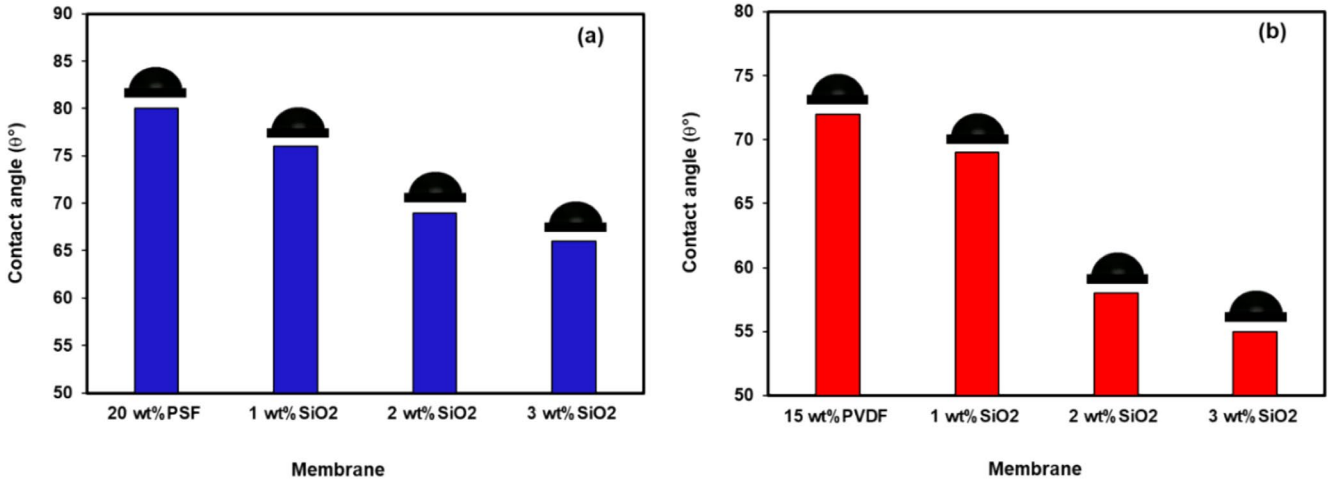

FIGURE 5 | Contact angle measurements of (a) 20 wt% PSF; 1 wt% SiO_2 NPs, 2 wt% SiO_2 NPs, 3 wt% SiO_2 NPs embedded PSF membrane surfaces. (b) 15 wt% PVDF; 1 wt% SiO_2 NPs, 2 wt% SiO_2 NPs, 3 wt% SiO_2 NPs embedded PVDF membrane surfaces. [Color figure can be viewed at wileyonlinelibrary.com]

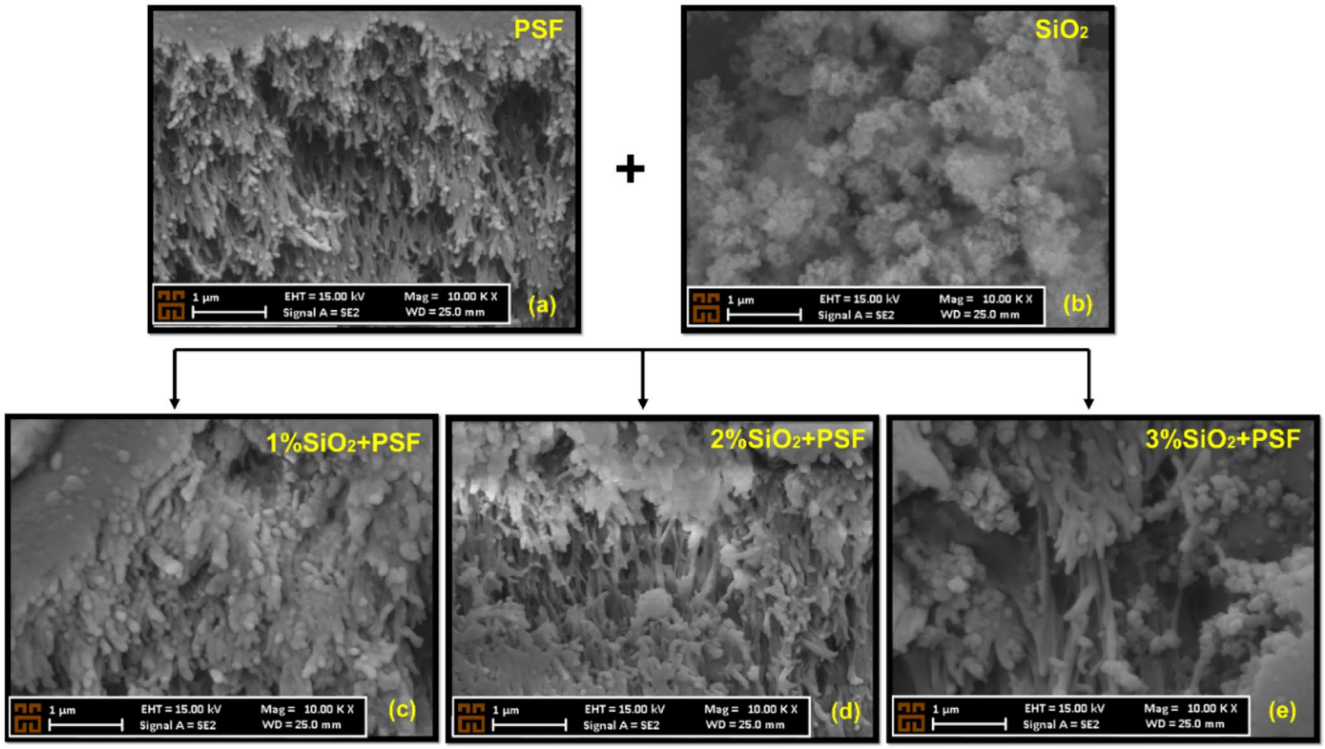

FIGURE 6 | The cross-section SEM images of (a) pristine PSF membrane, (b) SiO_2 NPs, (c–e) morphology of modified PSF membranes with different SiO_2 NPs concentrations. [Color figure can be viewed at wileyonlinelibrary.com]

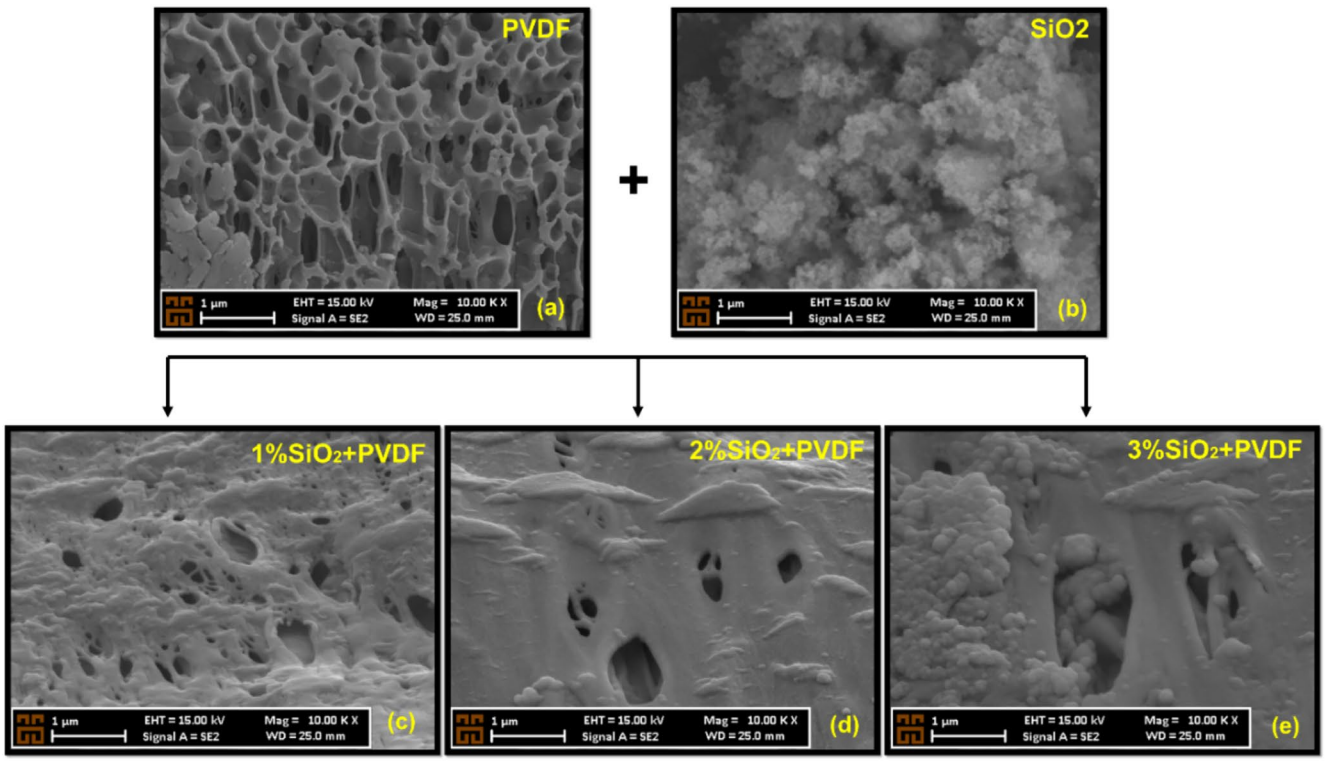

FIGURE 7 | The cross-section SEM images of (a) pristine PVDF membrane, (b) SiO_2 NPs, (c–e) morphology of modified PVDF membranes with different SiO_2 NPs concentrations. [Color figure can be viewed at wileyonlinelibrary.com]

than that of pristine PSF membrane [62]. Jafar discovered that when the amount of additives is increased up to 3 wt%, the mix membranes' pure water permeability rises. Higher hydrophilicity and improved pore structure of the blend membranes were the causes of the increase in pure water flux in the blend membranes [63].

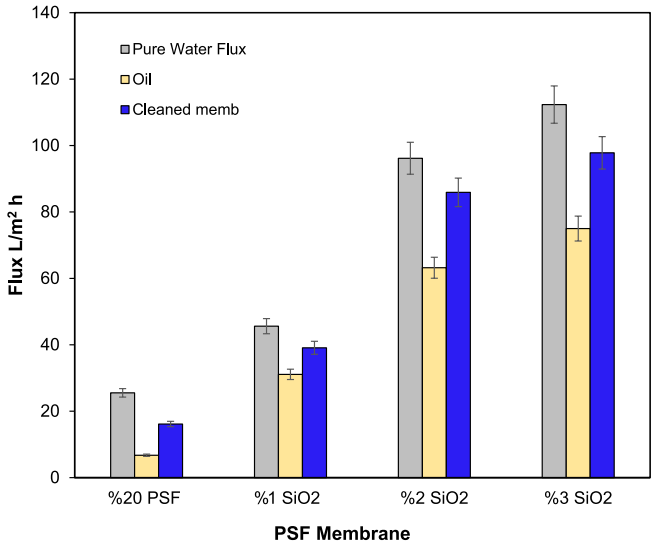

FIGURE 8 | Pure water, synthetic oily water, and cleaned membrane fluxes of 20 wt% PSF and three different concentrations of SiO_2 (1, 2, and 3 wt%) embedded membranes. [Color figure can be viewed at wileyonlinelibrary.com]

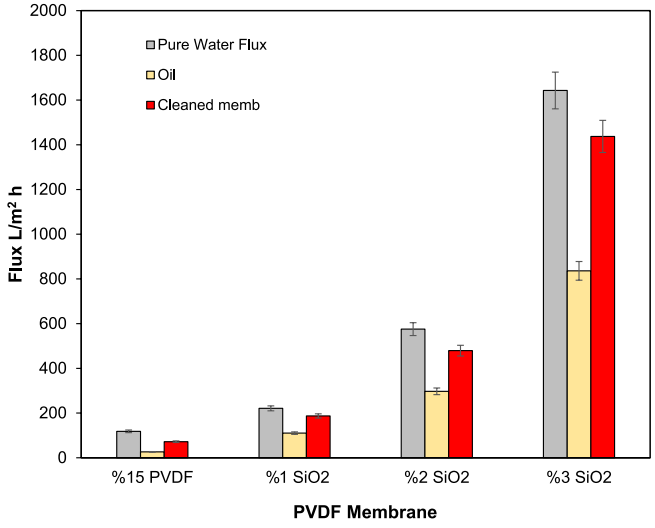

FIGURE 9 | Pure water, synthetic oily water, and cleaned membrane fluxes of 15 wt% PVDF and three different concentrations of SiO_2 (1, 2, and 3 wt%) embedded membranes. [Color figure can be viewed at wileyonlinelibrary.com]

The pristine water fluxes of PVDF, PVDF+1% SiO_2, PVDF+2% SiO_2, and PVDF+3% SiO_2 were determined at 5 bar using a dead-end filtration system. The results of pristine water flux from membranes are shown in Figure 9. The pristine water fluxes of PVDF, PVDF/1% SiO_2, PVDF+2% SiO_2, and PVDF+3% SiO_2 are 118.3, 221.1, 575.5, and 1642.9 $L\,m^{-2}h^{-1}$, respectively. As can be seen, the water flux for PVDF/ SiO_2 membrane increased from 118.3 to 1642.9 $L\,m^{-2}h^{-1}$ by the addition of SiO_2 from 1% to 3%. Similar findings were reported by Ngang, who discovered that membrane pure water fluxes increased when SiO_2 concentration increased from 57 to 93.86 L/m^2h. Theoretically, improved hydrophilicity and pore enlargement are the main reasons for membrane flux enhanced [64].

Figures 8 and 9 show pure water flow measurements before and after synthetic oily water filtration, as well as oily water fluxes for PSF, PVDF, PSF/SiO_2, and PVDF/SiO_2 membranes. When compared to pure water flux, oily water flux reduced significantly. Membrane fouling was the most common result of this flow reduction. Adsorption and deposition of oil droplets on the membrane surface occurred rapidly, resulting in membrane fouling. Membranes were cleansed with purified water for 20 min. Following that, flux recovery was computed to express the membranes' antifouling resistance with FRR [65].

4.6 | Oil Rejection of the (PSF/SiO_2) and (PVDF/SiO_2) Membranes

PVDF has a non-polar character due to its fluorinated structure, which leads to strong hydrophobicity. This property contributes to effective oil rejection by repelling oil droplets and limiting their adsorption on the membrane surface. Although PSF is hydrophobic, it can interact with water due to the polar sulfone group in its structure and allow oil permeability. SiO_2 NPs have been shown to affect the surface charge of the membrane. The negatively surface charged SiO_2 NP attracted water molecules while repelling non-polar oil molecules. Thus, it has been shown to improve oil rejection.

Figure 10 shows that the presence of nanoparticles improves oil rejection due to their molecular sieve capabilities. On the other side, the PSF membrane without SiO_2 has the lowest rejection performance, at 30.46%. The PVDF and PSF membranes with 2% SiO_2 had the highest oil removal effectiveness, at 94.05% and 92.16%, respectively.

Table 3 shows the separation performance of membranes (PSF, PVDF) with SiO_2 for oil–water emulsions. The oil rejection rates in this study are comparable to a number of other membranes described in the references. This shows that using SiO_2 NPs are the most promising technique for producing high-performance membranes for oily wastewater separation.

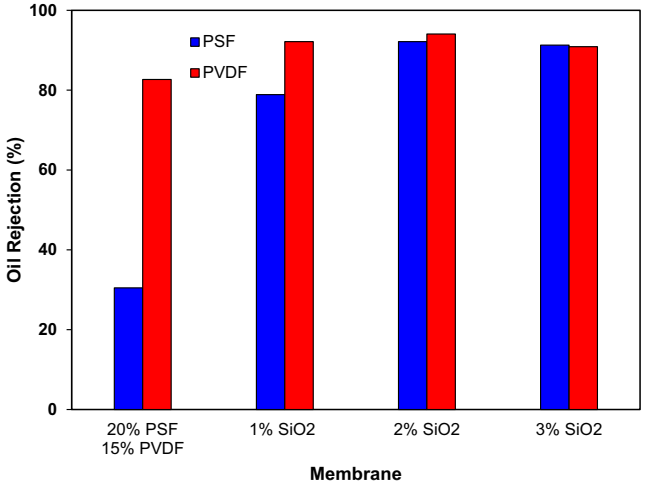

FIGURE 10 | Oil rejection rate of PSF, PVDF, PSF/SiO_2, and PVDF/SiO_2 membranes. [Color figure can be viewed at wileyonlinelibrary.com]

In comparison to previous studies on membrane-based oil filtration, this study demonstrates competitive oil rejection efficiencies, particularly with the PVDF/SiO_2 (94.1%) and PSF/SiO_2 (92.2%) membranes. While some studies report higher rejection rates (e.g., > 98% for PVDF/SiO_2 with additives like PVP and DMAc), these typically use oils such as n-hexane, vegetable oil, or diesel, which differ from the aging hydraulic oil tested in this study. The 10-cycle testing in this study is consistent with prior studies' cycle ranges of 5–30 cycles, demonstrating that the membranes in this study work well over numerous filtration cycles. Overall, the results are promising, particularly for the filtration of more complex oils like aging hydraulic oil.

Additionally, this study highlights the performance differences between the two membrane types and offers valuable insights for selecting the most suitable materials for specific applications.

The oil rejection rate and cycle number of different treatment methods are listed in Table 4. The table provides a comparison of various treatment methods for oil–water separation, along with their respective oil rejection percentages,

TABLE 3 | Comparison of membranes based on SiO_2 for rejection of oil.

Name of membrane	Additives	Oil rejection (%)	Type of oil	Cycle	Ref.
PVDF/SiO_2 (electrospinning)	—	> 98	n-hexane Petroleum ether Vegetable oil Vacuum pump oil	30 times	[66]
PVDF/SiO_2 nanofibrous membrane	—	97.95 98.3 92.7 90.8	Octane Hexadecane Diesel oil Rapeseed Oil	—	[67]
PVDF/SiO_2	PVP, DMAc, $MgCl_2$	99.4	Soybean oil	3 times	[45]
PVDF/ SiO_2	PVP	> 97.4	(n-hexane, xylene, methylene chloride, linseed oil, and motor oil)	10 times	[68]
PVDF/SiO_2	—	98	Crude oil in salty solution	—	[64]
PVDF/ SiO_2	—	94.15	Hexadecane	5	[69]
PSF/ SiO_2	Tween 80	98	Palm oil	—	[46]
PSF/SiO_2	—	—	Hexane Kerosene Gasoline	—	[70]
PSF/SiO_2	—	92.2	Aging hydraulic oil	10 times	This study
PVDF/SiO_2	—	94.1	Aging hydraulic oil	10 times	This study

TABLE 4 | Comparison of oil rejection with different treatment methods.

Treatment methods	Type of oil	Oil rejection (%)	Cycle	Ref.
Adsorption	Sesame oil Peppermint oil	> 55 > 85	5 times	[71]
Biological treatment	Soybean oil	> 90	—	[72]
Electrochemical treatment	Crude oil	98	—	[73]
Microemulsions (MEs)	Diesel engine oil	84.3–86.8	6 times	[74]
Flotation	Soybean oil	> 80	—	[75]
Nanofibrous aerogel	Toluene Kerosene n-hexane	> 99	10 times	[76]
Membrane filtration (PSF/SiO_2)	Aging hydraulic oil	92.2	10 times	This study
Membrane filtration (PVDF/SiO_2)	Aging hydraulic oil	94.1	10 times	This study

treatment cycles. Some treatment methods don't include cycle number. The effects of two different composite membranes on rejection of oil and cycle effect were examined and compared in this study. Table 4 serves as a comprehensive overview of the performance of different treatment methods in separating various types of oils from water, providing valuable insights for applications in industry and environmental remediation.

4.7 | Antifouling Capacity of the (PSF/SiO_2) and (PVDF/SiO_2) Membranes

The super hydrophilic strategy had a significant effect on alleviating irreversible fouling, but was not appropriate for reversible fouling. It was reflected that the flux recovery rates (FRRs) of super hydrophilic membranes could be close to 100%, but the flux decline rates (DRs) were usually more than 40% [77].

As shown in Table 5, when SiO_2 NPs were added to PSF membranes, the FRR value increases to more than 85%. The FRR value of a pristine PSF membrane is approximately 63.2%. Consequently, it can be stated that SiO_2 addition significantly improves the anti-fouling properties of membranes. Similar result found by Wu et al. [62] and Yao et al. [34]. A higher FRR value indicated that SiO_2-containing membranes had superior antifouling properties than neat membranes. This could be because the resulting membranes included additional silica nanoparticle additions, which also increase their hydrophilicity [63].

In general, a lower DR indicates stronger resistance to oil rejection, while a higher FRR indicates better physical cleaning effectiveness. As a result, both a lower DR and a higher FRR suggest improved antifouling capabilities [78].

The experimental results showed that the antifouling capacity of the PSF and PVDF membranes coated with SiO_2 NPs were significantly improved. When compared to pristine PSF and PVDF membranes, these new modified PSF and PVDF membranes performed better in terms of water flux and flux recovery ratio (FRR%).

TABLE 5 | Oil rejection ratio (%), FRR (%), and DR (%) values of PSF, PSF/SiO_2, and PVDF, PVDF/SiO_2 membranes for synthetic oil/water emulsion filtration.

Membrane	Oil rejection (%)	DR (%)	FRR (%)
20% PSF	30.5	73.6	63.2
PSF + 1% SiO_2	78.8	31.8	85.7
PSF + 2% SiO_2	92.2	34.3	89.3
PSF + 3% SiO_2	91.3	33.2	87.1
15% PVDF	82.7	77.6	60.7
PVDF + 1% SiO_2	92.2	50.1	84.7
PVDF + 2% SiO_2	94.1	48.3	83.3
PVDF + 3% SiO_2	90.9	49.1	87.5

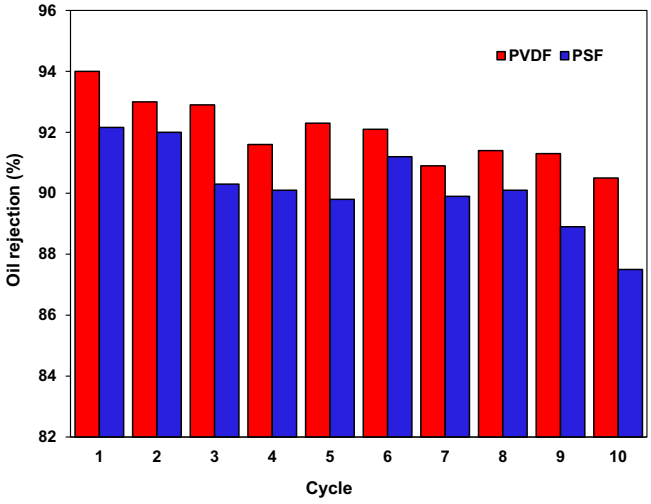

FIGURE 11 | The reusability test of the PVDF + SiO_2 and PSF + SiO_2 membranes. [Color figure can be viewed at wileyonlinelibrary.com]

4.8 | Cycling Experiment

PVDF and PSF membranes with 2% SiO_2 were also tested for separation efficiency using a dead-end filtration system in a continuous cycle separation. Equation (2) is used to calculate the oil rejection percentage for each cycle of PVDF and PSF membranes that include 2% SiO_2.

The results are shown in Figure 11. Even after 10 cycles, the rejection efficiencies of PVDF and PSF membranes with 2% SiO_2 remained steady, over 90% for PVDF, and more than 87% for PSF.

5 | Conclusion

The addition of SiO_2 NPs at various concentrations has been shown to increase the hydrophilicity of the membrane surface, resulting in improved water permeability and fouling resistance. Cycling studies have also shown that SiO_2 NPs can increase the durability and lifetime of the membrane by providing additional mechanical support and stability to the membrane structure. Furthermore, SiO_2 NPs are functionalized to selectively adsorb oil molecules, making them ideal for oil/water separation applications.

The water flux of the PSF/SiO_2 membrane surged from 25.3 to 112.3 $L\,m^{-2}\,h^{-1}$ with the SiO_2 NPs concentration rising from 1% to 3%.

PSF membranes doped with SiO_2 NPs have FRR values higher than 85%, which suggests a significant improvement in their antifouling characteristics. Consequently, the membrane's resistance to fouling is effectively maximized by the addition of SiO_2 NPs.

Membranes consisting of PVDF and PSF with 2% SiO_2 NPs exhibited higher oil removal efficiency with 94.05% and 92.16%, respectively.

PVDF and PSF membranes with 2% SiO_2 NPs continued to have constant removal efficiency even after 10 cycles.

Even after 10 cycles, the removal efficiencies of PVDF and PSF membranes with 2% SiO_2 NPs remained consistently high, with PVDF exceeding 90% and PSF surpassing 87%.

The addition of SiO_2 NPs to PSF membranes decreased the water contact angle from 79° to 67°, while the PVDF membranes decreased the water contact angle from 73° to 53°.

The experimental results demonstrate that the incorporation of SiO_2 NPs significantly improves oil rejection efficiency in both types of membranes. Comparative analysis shows performance differences between the two membrane types, suggesting that membrane material selection can significantly affect oil rejection efficiency.

Author Contributions

Dilek Senol-Arslan: conceptualization (lead), data curation (lead), formal analysis (lead), investigation (lead), methodology (equal), project administration (equal), writing – original draft (equal), writing – review and editing (equal). **Ayse Gul:** data curation (equal), formal analysis (lead), investigation (equal), methodology (equal), supervision (equal), writing – original draft (equal), writing – review and editing (equal).

Acknowledgments

We would like to express our deep gratitude to Prof. Dr. Niğmet Uzal for her constant guidance, support, and valuable feedback throughout the research process.

Conflicts of Interest

The authors declare no conflicts of interest.

Data Availability Statement

Data will be made available on request.

References

1. M. Cheryan and N. Rajagopalan, "Membrane Processing of Oily Streams. Wastewater Treatment and Waste Reduction," *Journal of Membrane Science* 151 (1998): 13–28.

2. J. Zhong, X. Sun, and C. Wang, "Treatment of Oily Wastewater Produced From Refinery Processes Using Flocculation and Ceramic Membrane Filtration," *Separation and Purification Technology* 32 (2003): 93–98.

3. M. Doble and A. K. Kruthiventi, "Industrial Examples," *Green Chemistry and Engineering* (Academic Press, 2007), 245–296.

4. J. Rubio, M. Souza, and R. Smith, "Overview of Flotation as a Wastewater Treatment Technique," *Minerals Engineering* 15 (2002): 139–155.

5. A. R. Pendashteh, A. Fakhru'l-Razi, S. S. Madaeni, L. C. Abdullah, Z. Z. Abidin, and D. R. A. Biak, "Membrane Foulants Characterization in a Membrane Bioreactor (MBR) Treating Hypersaline Oily Wastewater," *Chemical Engineering Journal* 168 (2011): 140–150.

6. R. K. Gupta, G. J. Dunderdale, M. W. England, and A. Hozumi, "Oil/Water Separation Techniques: A Review of Recent Progresses and Future Directions," *Journal of Materials Chemistry A* 5 (2017): 16025–16058.

7. Q. Li, C. Kang, and C. Zhang, "Waste Water Produced From an Oilfield and Continuous Treatment With an Oil-Degrading Bacterium," *Process Biochemistry* 40 (2005): 873–877.

8. E. Yuliwati and A. Ismail, "Effect of Additives Concentration on the Surface Properties and Performance of PVDF Ultrafiltration Membranes for Refinery Produced Wastewater Treatment," *Desalination* 273 (2011): 226–234.

9. C. Garcia-Jares, E. Becerril-Bravo, L. Sanchez-Prado, J. P. Lamas, T. Dagnac, and M. Llompart, "Analysis of Different High Production Volume Chemicals and Their Chlorination By-Products in Waters by Ultrasound-Assisted Emulsification–Microextraction," *International Journal of Environmental Analytical Chemistry* 94 (2014): 1–15.

10. S. B. Joye, "Deepwater Horizon, 5 Years on," *Science* 349 (2015): 592–593.

11. E. Kintisch, "American Association for the Advancement of Science," 2010.

12. B. Dubansky, A. Whitehead, J. T. Miller, C. D. Rice, and F. Galvez, "Multitissue Molecular, Genomic, and Developmental Effects of the Deepwater Horizon Oil Spill on Resident Gulf Killifish (Fundulus Grandis)," *Environmental Science & Technology* 47 (2013): 5074–5082.

13. A. Panagopoulos and V. Giannika, "A Comprehensive Assessment of the Economic and Technical Viability of a Zero Liquid Discharge (ZLD) Hybrid Desalination System for Water and Salt Recovery," *Journal of Environmental Management* 359 (2024): 121057.

14. A. Panagopoulos and V. Giannika, "Techno-Economic Analysis (TEA) of Zero Liquid Discharge (ZLD) Systems for Treatment and Utilization of Brine via Resource Recovery," *Chemical Engineering and Processing Process Intensification* 200 (2024): 109773.

15. D. R. Rowe and I. M. Abdel-Magid, *Handbook of Wastewater Reclamation and Reuse*, 1st ed. (London, UK: CRC Press, 2020).

16. N. Mehranbod, M. Khorram, S. Azizi, and N. Khakinezhad, "Modification and Superhydrophilization of Electrospun Polyvinylidene Fluoride Membrane Using Graphene Oxide-Chitosan Nanostructure and Performance Evaluation in Oil/Water Separation," *Journal of Environmental Chemical Engineering* 9 (2021): 106245.

17. L. Yan, X. Yang, Y. Zhao, et al., "Bio-Inspired Mineral-Hydrogel Hybrid Coating on Hydrophobic PVDF Membrane Boosting Oil/Water Emulsion Separation," *Separation and Purification Technology* 285 (2022): 120383.

18. E. Fikri, I. A. Sulistiawan, A. Riyanto, and A. E. Saputra, "Neutralization of Acidity (pH) and Reduction of Total Suspended Solids (TSS) by Solar-Powered Electrocoagulation System," *Civil Engineering Journal* 9 (2023): 1160–1172.

19. Y. Liu, R. Wei, O. Lin, et al., "Enhanced Hydrophilic and Antipollution Properties of PES Membrane by Anchoring SiO2/HPAN Nanomaterial," *ACS Sustainable Chemistry & Engineering* 5 (2017): 7812–7823.

20. Y. Tang, X. Hu, Y. Liu, Y. Chen, F. Zhao, and B. Zeng, "An Antifouling Electrochemiluminescence Sensor Based on Mesoporous CuO2@SiO_2/Luminol Nanocomposite and Co-Reactant of Ionic Liquid Functionalized Boron Nitride Quantum Dots for Ultrasensitive NSE Detection," *Biosensors and Bioelectronics* 214 (2022): 114492.

21. N. A. Chudasama, V. Polisetti, T. K. Maity, A. Reddy, and K. Prasad, "Preparation of Seaweed Polysaccharide Based Hydrophobic Composite Membranes for the Separation of Oil/Water Emulsion and Protein," *International Journal of Biological Macromolecules* 199 (2022): 36–41.

22. S. Zinatloo-Ajabshir and M. Salavati-Niasari, "Preparation of Magnetically Retrievable $CoFe_2O_4$@SiO_2@$Dy_2Ce_2O_7$ Nanocomposites as Novel Photocatalyst for Highly Efficient Degradation of Organic Contaminants," *Composites Part B: Engineering* 174 (2019): 106930.

23. H. M. Mousa, H. S. Fahmy, G. A. Ali, H. N. Abdelhamid, and M. Ateia, "Membranes for Oil/Water Separation: A Review," *Advanced Materials Interfaces* 9 (2022): 2200557.

24. H. Etemadi, S. Afsharkia, S. Zinatloo-Ajabshir, and E. Shokri, "Effect of Alumina Nanoparticles on the Antifouling Properties of Polycarbonate-Polyurethane Blend Ultrafiltration Membrane for Water Treatment," *Polymer Engineering & Science* 61 (2021): 2364–2375.

25. G. Hosseinzadeh, A. Sadeghiazar Sharabiani, M. Hermani, et al., "Construction of PVC/PVA WO3 3D Nanostructure Thin Film Nanocomposite for Treatment of Oil Refinery Wastewater," *Journal of Polymers and the Environment* 32 (2024): 1879–1891.

26. N. Ahmad, C. Leo, A. Ahmad, and W. Ramli, "Membranes With Great Hydrophobicity: A Review on Preparation and Characterization," *Separation and Purification Reviews* 44 (2015): 109–134.

27. W. Fu and W. Zhang, "Chemical Aging and Impacts on Hydrophilic and Hydrophobic Polyether Sulfone (PES) Membrane Filtration Performances," *Polymer Degradation and Stability* 168 (2019): 108960.

28. R. M. De Vos, W. F. Maier, and H. Verweij, "Hydrophobic Silica Membranes for Gas Separation," *Journal of Membrane Science* 158 (1999): 277–288.

29. P. Xu, X. Kong, X. Chen, K. Fu, M. Qiu, and Y. Fan, "Suitable Membrane Absorption Mode for Diluted Gas Absorption—Hydrophobic or Hydrophilic," *Separation and Purification Technology* 298 (2022): 121646.

30. S. Chaudhari, S. Jo, M. Shon, S. Nam, and Y. Park, "Hydrophobic Enrichment-Induced Augmentation of NH2-UiO-66 Particle Interactions for Enhanced Pervaporation Performance of Polydimethylsiloxane Membrane," *Journal of the Taiwan Institute of Chemical Engineers* 157 (2024): 105416.

31. M. Pyo, S. Jeong, J. H. Kim, M. J. Jeon, and E.-J. Lee, "Hydrophobicity and Membrane Distillation Performance of Glass Fiber Membranes Modified by Dip Coating of Pure PDMS," *Journal of Environmental Chemical Engineering* 12 (2024): 112534.

32. F. Ebrahimi, S. R. Nabavi, and A. Omrani, "Fabrication of Hydrophilic Special Sandwich Structure of PAN/GO/SiO_2 Electrospun Membrane Decorated With SiO_2 Nanoparticles for Oil/Water Separation," *Journal of Water Process Engineering* 48 (2022): 102926.

33. J. K. George and N. Verma, "Super-Hydrophobic/Super-Oleophilic Carbon Nanofiber-Embedded Resorcinol-Formaldehyde Composite Membrane for Effective Separation of Water-in-Oil Emulsion," *Journal of Membrane Science* 654 (2022): 120538.

34. Y. Yao, B. Zhang, M. Jiang, et al., "Ultra-Selective Microfiltration SiO_2/Carbon Membranes for Emulsified Oil-Water Separation," *Journal of Environmental Chemical Engineering* 10 (2022): 107848.

35. S. Z. Zakuwan, I. Ahmad, N. Abu Tahrim, and F. Mohamed, "Functional Hydrophilic Membrane for Oil–Water Separation Based on Modified Bio-Based Chitosan–Gelatin," *Polymers* 13 (2021): 1176.

36. M. Mansha, B. Salhi, S. Ali, S. A. Khan, and N. Baig, "Novel Procaine-Based Gemini Zwitterion Incorporated PVDF Membranes for Efficient Treatment of Oily Wastewater," *Journal of Environmental Chemical Engineering* 10 (2022): 107935.

37. Y. Liu, J. Liu, Z. Wang, Y. Yuan, J. Hua, and K. Liu, "Robust and Durable Superhydrophobic and Oil-Absorbent Silica Particles With Ultrahigh Separation Efficiency and Recyclability," *Microporous and Mesoporous Materials* 335 (2022): 111772.

38. S. Basak, S. Barma, S. Majumdar, and S. Ghosh, "Role of Silane Grafting in the Development of a Superhydrophobic Clay-Alumina Composite Membrane for Separation of Water in Oil Emulsion," *Ceramics International* 48 (2022): 26638–26650.

39. C. Wei, F. Dai, L. Lin, et al., "Simplified and Robust Adhesive-Free Superhydrophobic SiO_2-Decorated PVDF Membranes for Efficient Oil/Water Separation," *Journal of Membrane Science* 555 (2018): 220–228.

40. Y. Liu, Z. Yu, Y. Peng, L. Shao, X. Li, and H. Zeng, "A Novel Photocatalytic Self-Cleaning TiO_2 Nanorods Inserted Graphene Oxide-Based Nanofiltration Membrane," *Chemical Physics Letters* 749 (2020): 137424.

41. B. A. Gani, N. Asmah, C. Soraya, et al., "Characteristics and Antibacterial Properties of Film Membrane of Chitosan-Resveratrol for Wound Dressing," *Emerging Science Journal* 7 (2023): 821–842.

42. D. Senol-Arslan, "Isotherms, Kinetics and Thermodynamics of Pb(Ii) Adsorption by Crosslinked Chitosan/Sepiolite Composite," *Polymer Bulletin* 79 (2022): 3911–3928.

43. F. Tang, D. Wang, C. Zhou, et al., "Natural Polyphenol Chemistry Inspired Organic-Inorganic Composite Coating Decorated PVDF Membrane for Oil-in-Water Emulsions Separation," *Materials Research Bulletin* 132 (2020): 110995.

44. S. Rasouli, N. Rezaei, H. Hamedi, S. Zendehboudi, and X. Duan, "Superhydrophobic and Superoleophilic Membranes for Oil-Water Separation Application: A Comprehensive Review," *Materials & Design* 204 (2021): 109599.

45. Q. Xu, Y. Chen, T. Xiao, and X. Yang, "A Facile Method to Control Pore Structure of PVDF/SiO_2 Composite Membranes for Efficient Oil/Water Purification," *Membranes* 11 (2021): 803.

46. A. Ahmad, M. Majid, and B. Ooi, "Functionalized PSf/SiO_2 Nanocomposite Membrane for Oil-In-Water Emulsion Separation," *Desalination* 268 (2011): 266–269.

47. Y. Xu, X. Zeng, L. Qiu, and F. Yang, "2D Nanoneedle-like ZnO/SiO_2 Janus Membrane With Asymmetric Wettability for Highly Efficient Separation of Various Oil/Water Mixtures," *Colloids and Surfaces A: Physicochemical and Engineering Aspects* 650 (2022): 129352.

48. J. Cui, Z. Zhou, A. Xie, et al., "Bio-Inspired Fabrication of Superhydrophilic Nanocomposite Membrane Based on Surface Modification of SiO_2 Anchored by Polydopamine Towards Effective Oil-Water Emulsions Separation," *Separation and Purification Technology* 209 (2019): 434–442.

49. O. Dkhissi, A. El Hakmaoui, S. Souabi, M. Chatoui, A. Jada, and M. Akssira, "Treatment of Vegetable Oil Refinery Wastewater by Coagulation—Flocculation Process Using the Cactus as a Bio—Flo c Culant," *Journal of Materials and Environmental Science* 9 (2018): 18–25.

50. M. A. Ibrahim, M. Z. Jaafar, M. A. M. Yusof, C. A. Shye, and A. K. Idris, "Influence of Size and Surface Charge on the Adsorption Behaviour of Silicon Dioxide Nanoparticles on Sand Particles," *Colloids and Surfaces A: Physicochemical and Engineering Aspects* 674 (2023): 131943.

51. T. Diedrich, A. Dybowska, J. Schott, E. Valsami-Jones, and E. H. Oelkers, "The Dissolution Rates of SiO_2 Nanoparticles as a Function of Particle Size," *Environmental Science & Technology* 46 (2012): 4909–4915.

52. B. Ozbey-Unal, C. Balcik, and B. Van der Bruggen, "Development of a Novel Hydrophilic SiO2/PVDF Janus Membrane via Different Modification Methods for Robust Antiwetting and Antifouling Membrane Distillation," *Journal of Water Process Engineering* 54 (2023): 104021.

53. D. Senol-Arslan, A. Gul, N. Dizge, K. Ocakoglu, and N. Uzal, "The Different Impacts Ofg-C_3N_4 Nanosheets onPVDFandPSFultrafiltration Membranes for Remazol Black 5 Dye Rejection," *Journal of Applied Polymer Science* 140 (2023): e54514.

54. D. Senol-Arslan, A. Gül, N. Uzal, and E. Yavuz, "Ni-Zn Metal-Organic Framework Based Membranes for Rejection of pb(II) Ions," *Inorganic Chemistry Communications* 146 (2022): 110084.

55. T. Wu, B. Zhou, T. Zhu, et al., "Facile and Low-Cost Approach Towards a PVDF Ultrafiltration Membrane With Enhanced Hydrophilicity and Antifouling Performance via Graphene Oxide/Water-Bath Coagulation," *RSC Advances* 5 (2015): 7880–7889.

56. S. Saki, D. Senol-Arslan, and N. Uzal, "Fabrication and Characterization of Silane-Functionalized Na-Bentonite Polysulfone/Polyethylenimine Nanocomposite Membranes for Dye Removal," *Journal of Applied Polymer Science* 137 (2020): 49057.

57. A. Hosseinzadeh, P. R. Ranjbar, and A. Bozorg, "pH-Responsive P(AA-b-SBMA)-grafted Magnetic GO High-Performance Ultrafiltration Membrane With Improved Antifouling Tendency and Cleaning Efficiency," *Desalination* 574 (2024): 117299.

58. G. Karunakaran, R. Suriyaprabha, V. Rajendran, and N. Kannan, "Effect of Contact Angle, Zeta Potential and Particles Size on Thein Vitrostudies of Al_2O_3 and SiO_2 Nanoparticles," *IET Nanobiotechnology* 9 (2015): 27–34.

59. S. Banerjee, S. Kumar, A. Mandal, and T. K. Naiya, "International Journal of Oil," *Gas and Coal Technology* 15 (2017): 363.

60. A. Peyki, A. Rahimpour, and M. Jahanshahi, "Preparation and Characterization of Thin Film Composite Reverse Osmosis Membranes Incorporated With Hydrophilic SiO_2 Nanoparticles," *Desalination* 368 (2015): 152–158.

61. N. Hamzah, M. Nagarajah, and C. Leo, "Membrane Distillation of Saline and Oily Water Using Nearly Superhydrophobic PVDF Membrane Incorporated With SiO_2 Nanoparticles," *Water Science and Technology* 78 (2018): 2532–2541.

62. H. Wu, B. Tang, and P. Wu, "Development of Novel SiO_2–GO Nanohybrid/Polysulfone Membrane With Enhanced Performance," *Journal of Membrane Science* 451 (2014): 94–102.

63. M. A. Jafar Mazumder, P. H. Raja, A. M. Isloor, et al., "Assessment of Sulfonated Homo and Co-Polyimides Incorporated Polysulfone Ultrafiltration Blend Membranes for Effective Removal of Heavy Metals and Proteins," *Scientific Reports* 10 (2020): 7049.

64. H. Ngang, A. Ahmad, S. Low, and B. Ooi, "Preparation of PVDF/SiO_2 Composite Membrane for Salty Oil Emulsion Separation: Physicochemical Properties Changes and Its Impact on Fouling Propensity," *IOP Conference Series: Materials Science and Engineering* 206 (2017): 012083.

65. S. Saki and N. Uzal, "Preparation and Characterization of PSF/PEI/$CaCO_3$ Nanocomposite Membranes for Oil/Water Separation," *Environmental Science and Pollution Research* 25 (2018): 25315–25326.

66. S. Jiang, X. Meng, B. Chen, N. Wang, and G. Chen, "Electrospinning SuperhydrophobicSuperoleophilicPVDF-SiO_2 Nanofibers Membrane for Oil–Water Separation," *Journal of Applied Polymer Science* 137 (2020): 49546.

67. Y. Yang, Y. Li, L. Cao, Y. Wang, L. Li, and W. Li, "Electrospun PVDF-SiO_2 Nanofibrous Membranes With Enhanced Surface Roughness for Oil-Water Coalescence Separation," *Separation and Purification Technology* 269 (2021): 118726.

68. D. Gao, B. Xin, and M. A. A. Newton, "Preparation and Characterization of Electrospun PVDF/PVP/SiO_2 Nanofiber Membrane for Oil-Water Separation," *Colloids and Surfaces A: Physicochemical and Engineering Aspects* 676 (2023): 132153.

69. Y. Yang, Z. Guo, Y. Li, et al., "Electrospun Rough PVDF Nanofibrous Membranes via Introducing Fluorinated SiO_2 for Efficient Oil-Water Emulsions Coalescence Separation," *Colloids and Surfaces A: Physicochemical and Engineering Aspects* 650 (2022): 129646.

70. M. Obaid, G. M. Tolba, M. Motlak, et al., "Effective Polysulfone-Amorphous SiO_2 NPs Electrospun Nanofiber Membrane for High Flux Oil/Water Separation," *Chemical Engineering Journal* 279 (2015): 631–638.

71. R. M. Abdelhameed, R. S. Hasan, and H. Abdel-Gawad, "Removal of Carbaryl Residues From Sesame and Mint Oil Using Nano-Metal Organic Framework," *Journal of Molecular Structure* 1304 (2024): 137659.

72. X. Zhang, J. Cheng, X. Liu, et al., "Computer Assisted Design and Flow Field Analysis of a Multi-Tube Airlift Reactor for Biological Treatment of Oily Wastewater," *Journal of Water Process Engineering* 56 (2023): 104411.

73. L. C. Gobbi, I. L. Nascimento, E. P. Muniz, S. M. Rocha, and P. S. Porto, "Electrocoagulation With Polarity Switch for Fast Oil Removal From Oil in Water Emulsions," *Journal of Environmental Management* 213 (2018): 119–125.

74. H. Bi, C. N. Mulligan, K. Lee, et al., "Preparation, Characteristics, and Performance of the Microemulsion System in the Removal of Oil From Beach Sand," *Marine Pollution Bulletin* 193 (2023): 115234.

75. J. Xie, L. Liu, X. Huo, Q. Liu, X. Liu, and R. Duan, "Effect of Micro-Bubble Size and Dynamic Characteristics on Oil Removal Efficiency of the Flotation," *Separation and Purification Technology* 337 (2024): 126421.

76. X. Wang, Z. Liu, X. Liu, et al., "Ultralight and Multifunctional PVDF/SiO_2@GO Nanofibrous Aerogel for Efficient Harsh Environmental Oil-Water Separation and Crude Oil Absorption," *Carbon* 193 (2022): 77–87.

77. M. He, Z. Wang, Y. Zhang, P. Wang, X. He, and J. Ma, "Oil/Water Separation Membranes With Stable Ultra-High Flux Based on the Self-Assembly of Heterogeneous Carbon Nanotubes," *Journal of Membrane Science* 644 (2022): 120148.

78. S. Shi, K. Jian, M. Fang, J. Guo, P. Rao, and G. Li, "SiO_2 Modification of Silicon Carbide Membrane via an Interfacial In Situ Sol–Gel Process for Improved Filtration Performance," *Membranes* 13 (2023): 756.